Mitigation of indoor air pollution from air cleaners using a catalyst

Rebecca Mesburis[1], Madison Rutherford[1], Anne V. Handschy[1], Douglas A. Day[1], Melissa A. Morris[1], Anna C. Ziola[1], Zhe Peng[1,2], Joost A. de Gouw[1], Jose L. Jimenez[1 *]

[1] Department of Chemistry and Cooperative Institute for Research in Environmental Sciences, University of Colorado, Boulder, Colorado 80309, USA

[2] College of Environment and Climate, Guangdong−Hong Kong−Macau Joint Laboratory of Collaborative Innovation for Environmental Quality, Jinan University, Guangzhou 511443, China

* Email: jose.jimenez@colorado.edu

Abstract

The COVID-19 pandemic highlighted the importance of indoor air quality and the role of airborne transmission in disease spread. Heightened public awareness led to an increase in the commercialization and use of air cleaners. While several of these devices effectively disinfect the air, some also initiate chemical reactions that can worsen indoor air quality by generating ozone (O_3) and other harmful air pollutants. Here we demonstrate the use of a catalyst to mitigate both air cleaner-generated and ambient pollution in a real indoor environment. We deployed two real-time chemical ionization mass spectrometers alongside a suite of air quality analyzers to measure a wide range of volatile organic compounds (VOCs), other trace gases, and particles. We show the reduction of many indoor pollutants, including O_3, nitrogen oxides, formaldehyde, and other oxidized VOCs. We observe an increase in the concentrations of more reduced VOCs with catalyst use. We demonstrate that over 16 weeks of continuous operation, the clean air delivery rate of the catalyst for O_3 pollution declined linearly by 12.5%. These findings suggest that employing a dedicated catalyst could reduce indoor air pollution and enhance the human health benefits of air cleaners by minimizing the associated indoor air quality risks.

Keywords: Indoor Air Quality, Air Cleaners, Catalytic Reduction, Ozone, Volatile Organic Compounds, Particulate Matter, Clean Air Delivery Rate

Synopsis: This paper reports on the mitigation of ambient and air cleaner-generated indoor air pollution using a dedicated catalyst.

1. Introduction

Air pollution has been established as the second-leading risk factor for death worldwide, resulting in 8.1 million deaths in 2021.[1] People spend about 90% of their time indoors, where concentrations of some air pollutants are often considerably higher than typical outdoor concentrations.[2-3] Thus indoor environments play a primary role in human exposure to air pollution.[4] Exposure to gas-phase ozone (O_3), a common air pollutant, is associated with a range of negative health effects and increased mortality.[5-7] Notably, current evidence does not support a safe level of O_3 exposure.[5,8] Beyond its direct health impacts, exposure to both transient and stable oxidation products from O_3-initiated indoor chemistry (e.g., formaldehyde (HCHO), carbonyls, peroxides, ozonides) are an important human health concern.[9-12] The formation of secondary organic aerosol (SOA), a very harmful pollutant, represents a key group of stable compounds produced by O_3-driven chemistry indoors.[13-15] Formed SOA often consists of particles in the ultrafine (<0.1 μm) and fine (0.1-2.5 μm) size ranges ($PM_{2.5}$), which have stronger health effects per unit mass than O_3 itself.[15-17] Indoor concentrations of O_3 and $PM_{2.5}$ are often correlated to outdoor levels since they enter the indoor environment through infiltration and natural and mechanical ventilation systems.[18-20] While few indoor sources of O_3 exist, certain devices like printers, photocopiers, and some air cleaners can generate indoor O_3, ultimately increasing the potential for human exposure to O_3 and its indoor chemistry products.[20]

The COVID-19 pandemic raised global awareness of another important impact of indoor air quality: the importance of airborne disease transmission for SARS-CoV-2 and other respiratory pathogens.[21-23] The pandemic generated intense interest in air cleaners for air disinfection that could reduce the spread of airborne diseases indoors.[24-25] Some air cleaning/disinfecting technologies, such as electrostatic precipitators (ESPs) and germicidal ultraviolet at 222 nm (GUV222) lamps, have proven to be effective in disinfecting the air, but generate O_3 as a byproduct.[17, 26-30] GUV222 can also generate harmful secondary chemistry products including oxygenated volatile organic compounds (oVOCs) and SOA in typical indoor environments.[17, 31-34] Other oxidants (e.g., hydroxyl radicals) and HCHO represent additional common byproducts generated by indoor air cleaners.[35-37] Air cleaners are typically operated continuously in occupied spaces to enhance their effectiveness in reducing airborne transmission, and as a result, chemical byproducts from these devices may present a notable risk of exposure.[38]

The removal of indoor air pollutants including O_3 and HCHO has been of interest for decades. Various technologies such as catalytic and photocatalytic decomposition, activated carbon-based filtration, and passive (i.e., without a flow or fan) removal technologies have demonstrated O_3 removal.[39-43] Catalytic treatment of air to remove O_3 has been investigated, in particular through the use of manganese oxide (MnO_x)-based catalysts. MnO_x catalysts have garnered high interest owing to higher catalytic activity for O_3 removal over other transition metal oxides, as well as their low cost, environmental friendliness, and good overall stability.[39, 42, 44] One concern about this technology is its stability. Catalyst stability is complex and encompasses alterations in both the catalytic performance and its physicochemical characteristics. While there are many ways to represent catalyst stability, tracking performance decline is important for an initial stability assessment without probing degradation mechanisms.[45] It is well documented that pure MnO_x catalysts suffer from SO_2 poisoning and much effort has been dedicated to overcoming this issue through the modification of MnO_x catalysts with mixed oxides and metal-organic-frameworks, and optimizing catalyst morphology and structures.[46-49] With regards to indoor air, previous research on MnO_x-based catalysts has focused on the removal of HCHO considerably more than the removal of O_3.[50-54] In addition, the application of

MnO_x catalysts to real indoor environments remains underexplored, with unresolved questions about how the presence of other air pollutants might affect catalytic performance and the possible secondary chemistry products formed.[42, 53]

In this work, we evaluate the use of a MnO_x-based catalyst for the mitigation of indoor air pollution in both an atmospheric chamber and real office settings. We quantify the removal of several notable indoor air pollutants including O_3, nitrogen oxides (NO and NO_2), HCHO, and other volatile organic compounds (VOCs), and monitored the catalyst's effects on a large number of VOC and oVOC concentrations using two real-time chemical ionization mass spectrometers. We analyze the catalyst's durability over 16 weeks of continuous operation. Finally, the ability of the catalyst to abate O_3 pollution generated by an ESP and GUV222 lamps in a real office is explored.

2. Methods

2.1 Catalyst and Air Cleaner Information

The catalyst tested in this work was the PremAir BLD (BASF, China; Fig. S1). The catalyst consisted of an aluminum honeycomb structure (hexagons of side 1 mm) coated with a proprietary catalytic coating, which included MnO_x according to the manufacturer. The catalyst was designed for O_3 removal from indoor spaces. Two custom-sized catalyst pieces were obtained and installed in commercial portable high efficiency particulate air (HEPA) filter air cleaners, using their built-in fans to drive air flow through the catalyst. A smaller catalyst with dimensions 105 × 115 × 50 mm (macro-physical internal surface area ~ 0.67 m^2) was installed in a small, "personal" air cleaner (QT3, Smart Air Technology Co. Ltd, China; hereinafter "QT3") and used in the chamber and efficiency experiments. The QT3 arrived with a E11 filter and the catalyst was installed after the filter during all experiments to reduce soiling of the catalyst by PM (Fig. S2). A larger catalyst (262 × 304 × 30 mm, macro-physical internal surface area ~ 2.65 m^2) was installed in a room-sized air cleaner (AC350, Vornado Air LLC, USA; hereinafter "AC350") and used in the office experiments. The AC350 arrived with a True HEPA Filter and a Activated Carbon Filter (Vornado Air LLC). The HEPA and activated carbon filters were removed from the air cleaner.

Two commercial indoor air cleaning/disinfection methods were tested: an electrostatic precipitator (ESP) and GUV222 lamps. Both systems produce some O_3, and thus their operation together with the O_3 reduction catalyst is of high interest. The ESP was provided by the manufacturer and consisted of an ionization system with charged wires, a cylindrical metal collector surface, and pleated filter. The ESP was advertised to remove aerosols and have a flow of 175 to 300 $m^3\ h^{-1}$ depending on the fan speed and operative settings (300 $m^3\ h^{-1}$ = 5000 lpm). Two GUV222 lamps were used, both with the Ushio B1 Far UV-C 222 nm Excimer Lamp (Ushio America Inc., USA). One was the OSLUV Death Ray 222 nm (The OSLUV Project, USA) and the other was the FarUV Krypton-36 (Far UV Technologies, Inc., USA).

2.2 Teflon Chamber Experiments

Experiments were conducted in a well-characterized ~ 21 m^3 chamber constructed of 50 µm thick FEP Teflon at the University of Colorado-Boulder Environmental Chamber Facility.[55-56] Clean air (NO_x < 0.2 ppb; VOC < 50 ppb) was supplied to the chamber at 400 lpm using two AADCO 737-15A clean air generators at slightly positive pressure (1-2 Pa) for several hours

prior to each experiment. The chamber bag was filled until the differential pressure reached 3.5 Pa immediately prior to each experiment. O_3 was injected by flowing O_2 from a compressed gas tank (Table S1) and applying voltage to generate corona discharge using a BMT 802 N ozone generator (BMT Messtechnik GmbH, Germany). NO and NO_2 were injected from compressed gas tanks (Table S1). After each injection, the air in the chamber bag was mixed for about two minutes with a Teflon-coated mixing fan integrated inside the chamber. The catalyst was installed inside the chamber within the QT3 and mounted on a ring stand near a bottom corner of the chamber (Fig. S3).

2.3 Real Office Experiments

The durability of the catalyst was assessed. We aged the smaller catalyst by continuous operation (i.e., air flow through the material) in the QT3 for 16 weeks. The catalyst was aged in a university office ("Office A") typically occupied by five people during working hours.

Experiments aimed at investigating the indoor air quality impacts of the catalyst in a real indoor environment were conducted in a ~ 33 m^3 university office (4.0 × 2.7 × 3.1 m; "Office B") with an entrance door and two windows. The office was carpeted and fitted with typical office furniture including a desk and chair. To reduce variability from intermittent operation of the ventilation system, to imitate a low-ventilation situation similar to a home where disinfecting air cleaners are most impactful, and to increase the signal-to-noise of the measurements, the vents, windows, and entrance door were sealed with plastic film and/or tape (Fig. S4). Air change rates (ACRs) were quantified by measuring carbon dioxide (CO_2) decay. CO_2 from a compressed air tank (Table S1) was injected into the room and monitored with an Aranet4 sensor (SAFTehnika, Latvia). A box fan inside the office was turned on remotely for one minute after each CO_2 injection to ensure mixing. Figure S5 shows multiple time series of CO_2 decays and resulting ACRs. ACRs in the office varied from 0.14 h^{-1} to 0.57 h^{-1} with a mean of 0.26 h^{-1} during these measurements. The surface area to volume ratio accounting for contents of the room was 2.3 m^{-1}. These values are consistent with those previously reported in typical residences and offices.[57-58] The larger catalyst was installed inside the AC350 and placed in the office. Cyclic on/off operation of the catalyst was conducted in periods of several hours. The on/off operation allowed repeated chemical changes observed in the office space to be attributed to the use of the catalyst. The ESP and GUV222 lamps were used during some office experiments. The ESP was placed in the middle of the indoor office test space without any obstructions near its clean air output and operated at a constant speed (maximum setting). The two GUV222 lamps were placed high up in adjacent corners of the office and faced towards the middle of the room. The average fluence rate in the room was estimated at 2.4 μW cm^{-2}, which is slightly higher than the upper limit fluence rate in typical installations that comply with the ACGIH limit.[17] The catalyst and air disinfection devices were controlled remotely from outside the office using a PRO Switch (Digital Loggers Inc., USA).

Three office B experiments are described here. These included: (i) a five-day experiment with six-hour on/six-hour off cycling of the catalyst and (ii) two experiments with continuous catalyst cycling and an intermediate period of intermittent air disinfection/cleaning device operation. In the first set of the latter experiments, the catalyst cycled on/off every 4 h for 8 full cycles and the ESP operated continuously during the middle 4 cycles. In the second set, the catalyst cycled on/off every 6 h for 8 full cycles and the GUV222 lamps operated continuously during the middle 4 cycles.

2.4 Instrumentation

O_3 was monitored using a Thermo Scientific 49i O_3 Analyzer during chamber experiments and a 2BTech Model 205 Dual Beam O_3 Monitor during catalyst characterization and office experiments. Both O_3 instruments operate by UV light absorption at 254 nm, and were zeroed before and after each experiment using a carbon-cap (Whatman Inc., USA). NO and NO_2 were monitored using a Thermo Scientific Model 42i-TL TraceLevel NO_x Analyzer. The NO_x instrument operates by chemiluminescence and was zeroed with clean chamber air (which has been shown to have NO_x below the detection limit, $NO_x < 0.2$ ppb) and by overflowing the inlet with ultrahigh purity nitrogen (N_2) from a compressed gas tank (Table S1). HCHO was monitored using a Picarro G2307 cavity ringdown Gas Concentration Analyzer. Particles were measured using a scanning mobility particle sizer (SMPS; TSI models: 3080 electrostatic classifier, 3081 differential mobility analyzer (DMA), and 3776 condensation particle counter). The system was operated using a 3 L min^{-1} sheath flow and a 0.3 L min^{-1} sample flow. The size distributions were measured every 135 s and the number and volume concentrations were calculated by integrating over 16-685 nm mobility diameter. The DMA was calibrated with polystyrene latex spheres. The SMPS data was analyzed using custom software for particle size distributions in Igor Pro 9 (Wavemetrics, USA).[59]

2.4.1 Iodide ToF-CIMS

A Chemical Ionization Time-of-Flight Mass Spectrometer (ToF-CIMS, TOFWERK AG, Switzerland and Aerodyne Research, Billerica, USA) was used to measure various oxygenated and nitrogenated VOCs in high resolution with iodide (I^-) reagent ions (hereinafter the "I-CIMS" for short).[60] Tofware v4.0.2 in Igor Pro 9 was used for analyzing the I-CIMS data. Mass-to-charge ratio calibration was performed using 7 ions between *m/z* 61 and 491 with a resulting mean residual of 2 ppm. Peaks were assigned elemental formulas and time series calculations were performed in Tofware by fitting the determined customized peak shape to each of the assigned *m/z* values. The data was then normalized to one million total reagent ion [I^- + $I(H_2O)^-$] counts per second (cps), which is indicated by the units of normalized cps (ncps). Ion masses of interest were selected for further processing if they demonstrated variability during catalyst cycling (also applies for the Vocus processing, section 2.4.2 below). The I-CIMS was calibrated by injections of formic acid (HCOOH) to the chamber (Fig. S6). HCOOH (Table S1) was evaporated into the chamber using a glass bulb under N_2 flow and slight heat from a heat gun. As with the O_3 and NO_x chamber injections, the air in the chamber bag was mixed after each injection. HCOOH was injected in ~ 5 ppb increments at first and then in a few ~ 10 ppb increments to yield a calibrated HCOOH concentration range up to ~ 55 ppb. Signals that had identifiable changes by visual inspection of the catalyst cycles were summed (43 compounds). The HCOOH sensitivity was assumed for all species and applied to approximate the "bulk oxidized VOCs" as measured by the I-CIMS. The term bulk was used to mean the total signal using a single value for sensitivity. It is acknowledged that sensitivities for different species detected by the I-CIMS can vary by orders of magnitude and thus its bulk concentration is uncertain. Thus, bulk concentrations were strictly interpreted by focusing on the relative increases and decreases during air cleaner and catalyst operation.

2.4.2 Vocus Elf PTR-ToF-MS

A Vocus Elf Proton-Transfer-Reaction Time-of-Flight mass spectrometer (Vocus Elf PTR-TOF, TOFWERK AG; hereinafter "Vocus" for short) was used to measure VOCs in unit mass resolution (UMR).[61] The instrument is a compact PTR-TOF mass spectrometer. VOCs were ionized by reactions with H_3O^+ ions from a discharge and detected in a compact TOF MS with a mass resolution of 1000 (m/Δm).[62] The non-compact version of the instrument has been described in great detail in a previous publication.[63] The Vocus was zeroed using a zero-air generator and calibrated using a standard calibration gas mixture from Apel-Riemer Environmental, Inc. (USA) containing several VOCs (acetaldehyde, acetonitrile, acetone, acrylonitrile, isoprene, methyl ethyl ketone, benzene, toluene, chlorobenzene, o-xylene, α-pinene, phenol, 1,3,5-trimethylbenzene) every hour during data acquisition. Tofware v3.2.5 in Igor Pro 9 was used for processing the Vocus data. The *m/z* scale was calibrated using 6 ions between *m/z* 42 and 171 with a mean residual of 31 ppm. Sensitivities were linearly interpolated between hourly calibrations. For compounds included in the calibration gas mixture, the sensitivities were determined from the direct calibration. Otherwise, theoretical sensitivities were calculated using proton transfer reaction (PTR) rate constants (k_{PTR}) from the literature.[64-65] Although the Vocus can measure HCHO, owing to a strong humidity dependence, lower sensitivity, and positive interferences at high O_3 levels in PTR-MS, the Picarro measurements were used exclusively.[66-68] Signals that had identifiable changes by visual inspection of the catalyst cycles were summed (34 VOCs) and a bulk PTR sensitivity was applied to approximate the "bulk reduced VOCs" as measured by the Vocus. Note that HCHO was not included in the bulk calculation for either the bulk reduced or oxidized VOCs traces.

2.5 Calculation of Single-Pass Efficiencies and Clean Air Delivery Rates

To assess the efficiency of the catalyst, we determined the single pass efficiency (SPE) and clean air delivery rate (CADR) for pollution removal. SPE quantifies the catalyst's ability to reduce the concentration of a pollutant in a specific volume of air that passed through the catalyst once. Measurements for SPE_{O3} quantification were taken in an outdoor rooftop laboratory space, to allow a sufficient and constant background O_3 (Fig. S7). SPEs were then computed using Eq. (1):

$$SPE_{O_3} = \left(1 - \frac{O_{3\ out}}{O_{3\ in}}\right) \times 100\,\% \quad \textbf{(1)}$$

where $O_{3\ out}$ and $O_{3\ in}$ were the O_3 concentrations immediately downstream and upstream of the catalyst.

SPEs for other pollutants were estimated using the ratio of decay rates and the O_3 SPE using Eq. (2):

$$SPE_X = \frac{k_X}{k_{O_3}} \times SPE_{O_3} \quad \textbf{(2)}$$

where k_X and k_{O3} were the decay rates of pollutant X and O_3 determined during the chamber experiments and SPE_{O3} was the result from Eq. (1). Rate coefficients for the loss of O_3 and other pollutants due to catalyst operation or natural decay were calculated using an exponential fit.

CADR (m^3 h^{-1}) quantified how efficiently a pollutant present in the test space was removed by the catalyst, accounting for the volume of the test space and the pollutant decay in the absence of a catalyst ($k_{decay,\ catalyst\ off}$).[69] CADRs were determined using Eq. (3):

$$CADR = V(k_1 - k_2) \quad \textbf{(3)}$$

where V was the volume of the chamber and k_1 (k_2) was the rate coefficient determined with (without) catalyst operation. The CADR metric was used for the O_3 removal durability assessment of the catalyst.

3. Results and Discussion

3.1 Removal of Ozone, Formaldehyde, and Nitrogen Oxides

The catalyst efficiently removed O_3 in all scenarios tested: ambient single-pass, atmospheric chamber, and indoor office. Results from the catalyst characterization experiments are summarized in Fig. 1. Figure 1a shows the first order loss of O_3 in the Teflon chamber with catalyst operation. The decay rate and CADR were 2.3 h^{-1} and 48 m^3 h^{-1}, respectively, for the new catalyst as received (no aging). The O_3 decay curves from later experiments show that the ability of the catalyst to remove O_3 slightly decreased with catalyst age. Figure 1b characterizes the removal of O_3 in terms of SPE. SPE ranged from 90.8 to 96.6%, increasing with decreasing fan speed (at zero weeks of catalyst aging). As the fan speed decreases, the air has more time to interact with the catalyst material, thus increasing the efficiency. Figure 1c depicts the initial CADR and its decline with catalyst aging. $CADR_{O3}$ was 48, 45, and 42 m^3 h^{-1} at 0, 8, and 16 weeks of continuous real-world aging, respectively. Over the sixteen weeks of aging, $CADR_{O3}$ decreased by about 12.5% in a monotonic trend. At the end of the aging period, verification tests with the original and a newly purchased QT3 were conducted to ensure that the air cleaner fan or battery had not aged instead of the catalyst. It was determined that the extended use of the air cleaner components had made a smaller contribution for the decline in catalyst efficiency ($k_{original\ QT3} = 1.97 \pm 0.03$, $k_{new\ QT3} = 2.05 \pm 0.01$, uncertainties quoted are 2σ), meaning that at least ⅔ of the decline was due to the catalyst itself.

Figure 1d shows the removal of O_3 and HCHO by the catalyst in office B. During catalyst operation in the office, rapid and synchronous removal of O_3 and HCHO was observed (R^2 = 0.91 between their mixing ratios during this experiment). From the decay curves, it can be seen that O_3 and HCHO reached steady-state concentrations in about 1.5 hours (~ 3 and 12 ppb, respectively). After airflow through the catalyst was stopped, concentrations of both pollutants increased and approached steady-state.

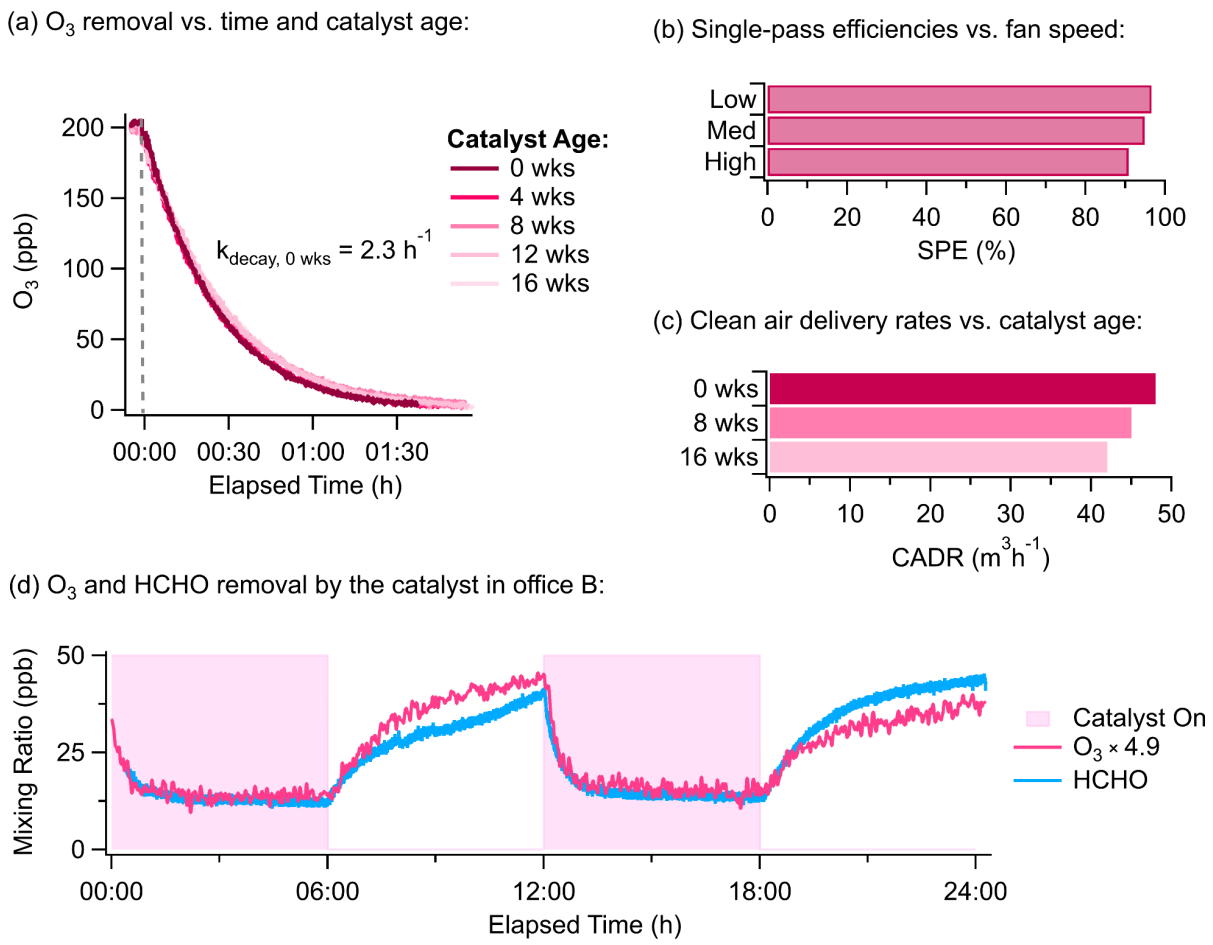

Figure 1: *Characterization of the catalyst: (a) O_3 removal versus time in the Teflon chamber at 0, 4, 8, 12, and 16 weeks of catalyst age, (b) single-pass efficiencies at 0 weeks aged with low, medium, and high fan speeds,(c) clean air delivery rates at 0, 8, and 16 weeks of catalyst age, and (d) removal of O_3 and HCHO in an indoor office due to operation of the catalyst.*

To assess the impact of the catalyst on additional indoor air pollutants, chamber experiments exposing the catalyst to NO and NO_2 were performed (Fig. 2). Figures 2a and 2b show the removal of NO and NO_2 in the chamber with catalyst operation. We estimated the SPEs to be 71.1% and 79.0% for NO and NO_2, respectively (for the new catalyst before any aging). Although aging the catalyst had a limited effect on O_3 removal performance, it had a larger impact on NO_x removal. For instance, the decay rate for NO decreased by about 22% after 7 weeks of catalyst aging (k_0 = 1.8 h^{-1} and k_7 = 1.4 h^{-1} where k_x represents the decay rate at x weeks). Catalyst age also impacted the observed products for NO_2 removal by the catalyst. Figure 2c shows that when the catalyst was used to remove ~ 50 ppb of NO_2 at 0 weeks aged no NO formation was observed. In contrast, Figure 2d shows that at 7 weeks of aging the catalyst removes NO_2 and forms NO at an approximate 2:1 ratio. This relationship was confirmed by several repeats of the experiment at 7 weeks of aging with varying initial NO_2 concentrations ($k_{NO2,\ 7\ weeks}$ = 1.8 to 1.9 h^{-1}) (Fig. S8). It is possible that in both the 0 and 7 week tests NO_2 was converted to NO but during the latter test the NO removal slowed due to the catalyst age which allowed for NO accumulation. This indicates that although the catalyst persisted in its ability to

reduce O_3, NO, and NO_2 over weeks of continuous use, it became less efficient over time, with different rates of aging for different pollutants.

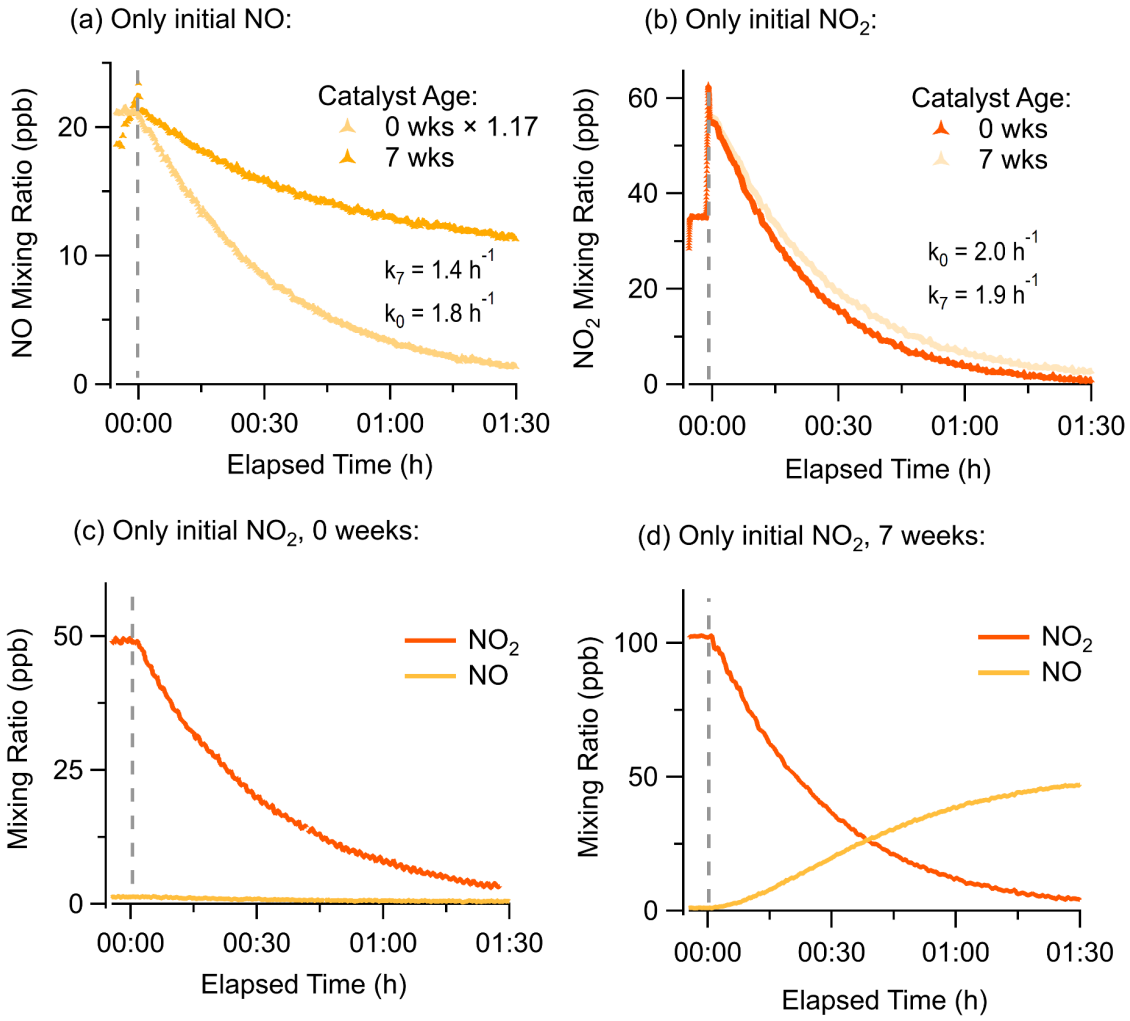

Figure 2: *Mitigation of NO_x pollution using the catalyst in the Teflon chamber. (a) Reduction of NO at 0 and 7 weeks of catalyst age. (b) Reduction of NO_2 at 0 and 7 weeks of catalyst age. (c) Removal of NO_2 at 0 weeks of catalyst age without consequent NO production. (d) Removal of NO_2 at 7 weeks of catalyst age with NO production.*

Impacts to nitrogen-containing compounds were further examined using the time series measured by the I-CIMS in office B of several indoor-relevant species including HONO, HNO_3, and N_2O_5. There were no identifiable changes to HONO or HNO_3 when the catalyst cycled. We did identify a small increase in N_2O_5 with catalyst operation (Fig. S9). Using previously reported relative sensitivities of HCOOH and N_2O_5, we estimated this change in N_2O_5 to correspond to an increase on the order of part per quadrillion levels during the 6-hour periods of catalyst use.[60]

3.2 Removal and Formation of Volatile Organic Compounds

We studied the effect of the catalyst on the removal and formation of VOCs in a real indoor environment, as exposure to VOCs can be linked to negative health effects.[70-71] VOC levels were monitored in office B while cycling the catalyst on and off. Figure 3a-b shows averaged difference spectra between the catalyst-off and the catalyst-on periods. The horizontal dashed lines indicate the signal level above which changes in concentration with catalyst use were visually discernible in VOC time series (hereinafter the detection limit for changes "DLC" line for short). Figure 3a (3b) shows that signals of reduced (oxidized) VOCs tended to increase (decrease) during catalyst operation. Figure 3c shows diurnal variation (averaged over the 5 days) time series for chemical species that showed detectable fluctuations with catalyst use. The top left panel displays the bulk reduced and oxidized VOC changes with catalyst use, and highlights the reproducibility and synchronicity of the reduced and oxidized VOC behavior observed over concurrent cycles. We also included diurnal time series plots for two reduced VOCs measured in UMR by the Vocus and three oxidized VOCs measured in high resolution by the I-CIMS. The protonated elemental formulas (and likely compounds) associated with the reduced VOCs displayed in Fig. 3c are: *m/z* 79 ($C_6H_7^+$ from benzene) and *m/z* 93 ($C_7H_9^+$ from toluene). Both reduced VOCs increased on the order of a ppb per 6-hour catalyst activity period over the five day experiment. In contrast, the displayed oxidized VOCs decreased and changed more substantially over each 6-hour catalyst-on period. HCOOH decreased on the order of ~ 30 ppb when the catalyst was on (Fig. 3c). Lactic acid ($C_3H_6O_3$), glycolic acid ($C_2H_4O_3$), and the other examined oVOCs above the DLC line followed the same decreasing trend (Fig. 3b-c).

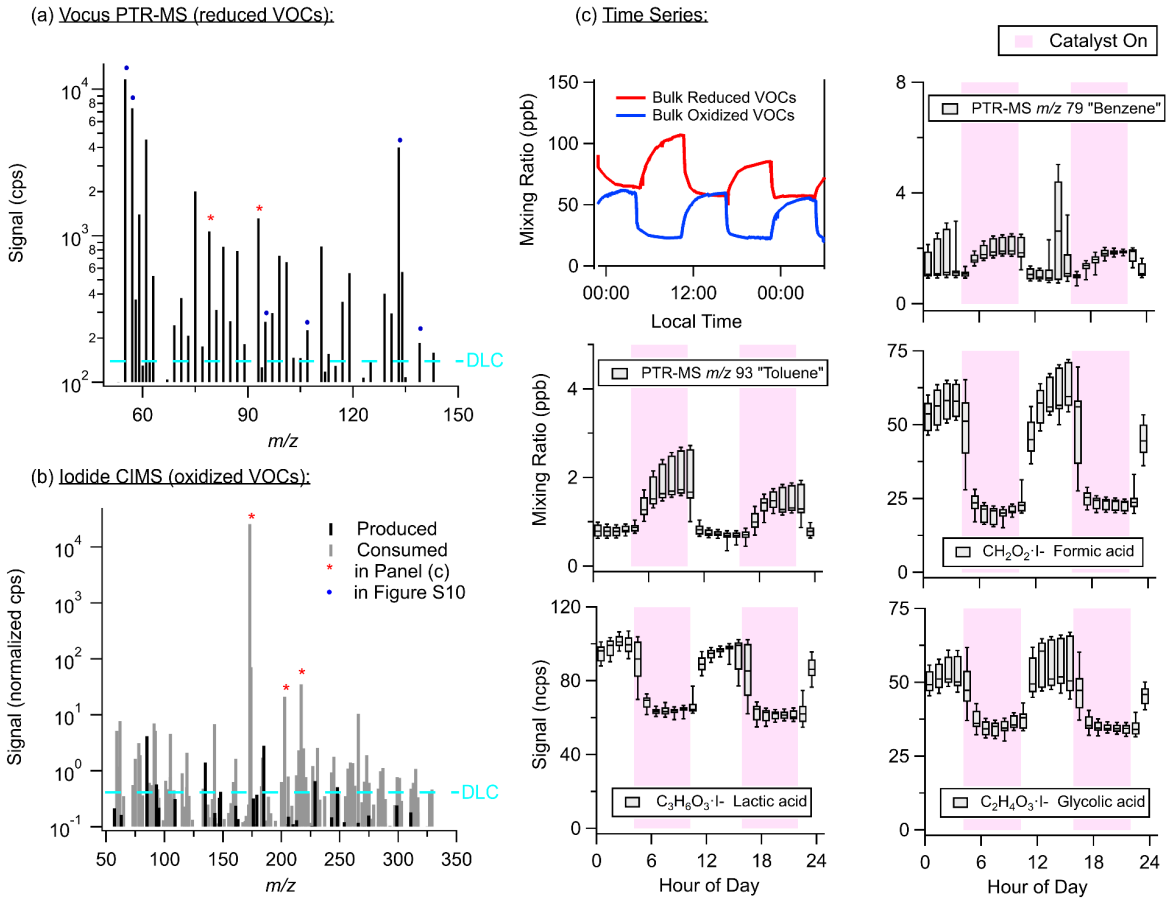

Figure 3*: Removal and formation of VOCs during catalyst use over five days of continuous measurement in office B. (a-b) The resulting signals from the difference spectra of the averaged catalyst on and off periods were presented as a function of m/z on a positive y-axis and colored by increase or reduction when the catalyst was on. Horizontal dashed lines indicated the level below at which no changes were identifiable by visual inspection of the corresponding diurnal cycles and is referred to as the detection limit for changes "DLC" line. (a) Increase of VOCs during catalyst operation as measured by the Vocus PTR-MS and (b) Mostly decreases with a few increases in VOCs during catalyst operation as measured by the I-CIMS. (c) Top left: Time series of the bulk reduced and oxidized VOCs. (c) Diurnal time series plots of several PTR-MS unit masses and I^- molecular ions that varied strongly with catalyst operation. Boxes represented data from the first to third quartiles and whiskers represented data from the 9th to 91st percentiles. The horizontal line markers represent the median values.*

Some of the prominent reduced VOC species (i.e., above the DLC line) demonstrated unclear time series variations. This uncertainty was observed in reduced VOC species that are typically of relevance to indoor air. The changes at *m/z* 59, 95, and 137, which are typically associated with acetone, phenol, and α-pinene and other monoterpenes, respectively, did not show strong variation with catalyst use (Fig. S10). Others (*m/z* 57, 107, 133) did show a consistent yet small increase with catalyst use. Importantly, most of these changes in reduced VOCs were also of a low initial concentration and remained below ~ 4 ppb during repeated catalyst use cycles. Although not all prominent reduced VOC signals demonstrated consistent behavior with catalyst operation, the sum of these reduced VOC signals and the medians of the sum explicitly increased with catalyst use (Fig. S11). We conclude that the catalyst does not appear to change total VOC concentration, but it does cause changes to the overall VOC composition. These changes may or may not lead to deteriorated air quality.

3.3 Mitigation of Air Cleaner-Generated Pollution

Next, we studied the mitigation of pollution generated by two air cleaning / disinfection methods in office B. The catalyst effectively reduced O_3 produced by both the ESP and GUV222 lamps, maintaining O_3 concentrations in the office at ~ 3 and ~ 5 ppb during catalyst operation, respectively (Fig. 4). Figure 4a shows that the ESP generated O_3 and substantially reduced particle number and volume concentrations. Figure 4b shows that the GUV222 lamps generated O_3 and increased particle number and volume concentrations, with new particle formation (NPF) occurring during the later periods when the GUV222 lamps were on and the catalyst was off. This indicates that the catalyst was useful in suppressing both NPF and particle mass increases induced by the GUV222 lamps. Together, these findings suggest that although these disinfection technologies produce indoor air pollutants, their combined use with a dedicated catalyst helps to mitigate the generated O_3 and PM.

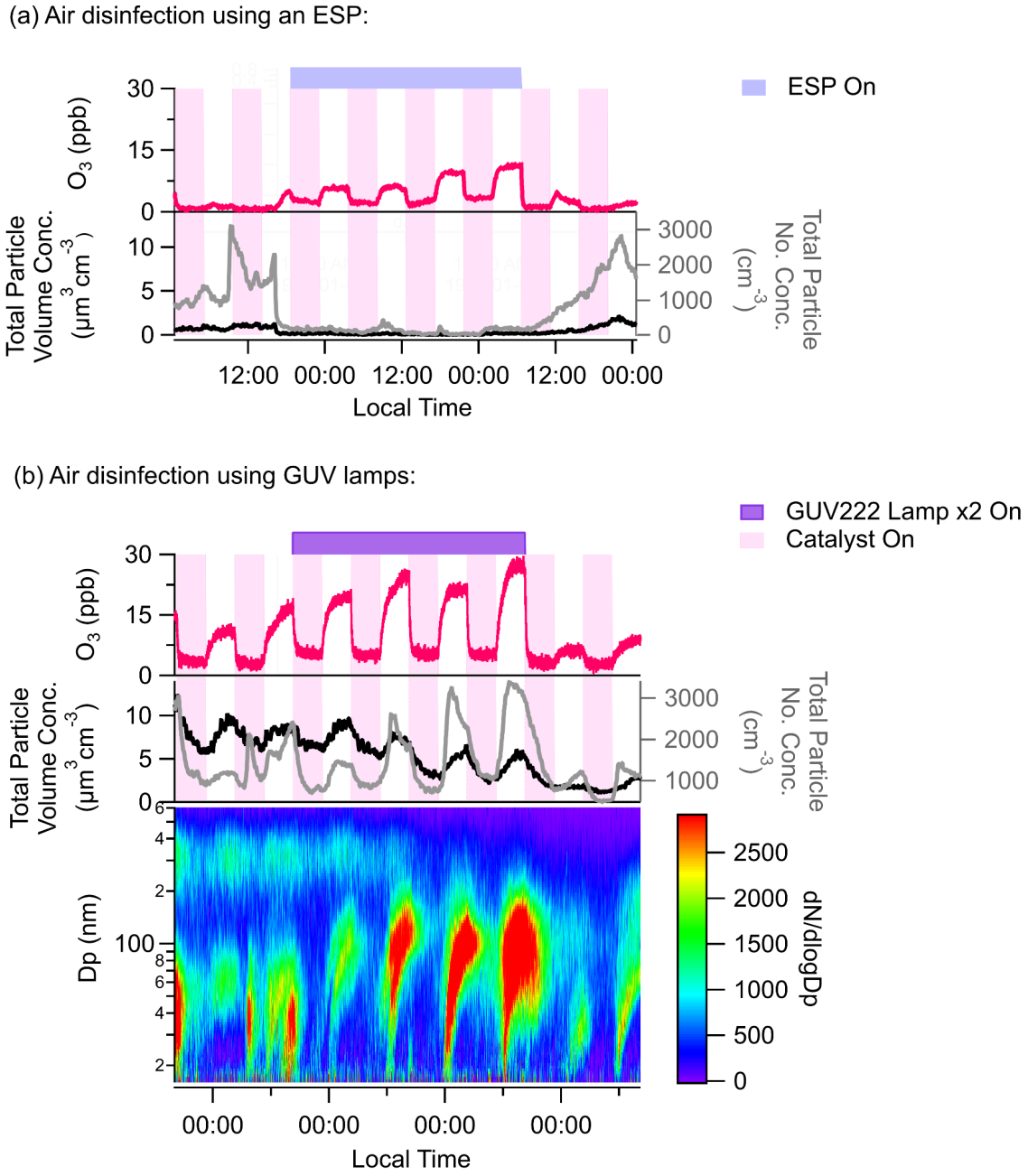

Figure 4: *Time series of O_3, total particle volume, and total particle number concentrations during continuous cycling of the catalyst with (a) an intermediate period of ESP operation and (b) an intermediate period of GUV222 lamp operation. The aerosol particle number size distributions are shown as an image plot for the GUV222 experiment.*

3.4 Implications

The findings of this study demonstrate substantial reductions in key indoor air pollutants using a catalyst, including O_3, HCHO, NO, NO_2, PM, and many oVOCs. It is useful to note the reduction of NO and NO_2, which are commonly emitted by gas stoves and other burning

appliances, since alternative indoor air treatment methods like HEPA filters and activated charcoal do not remove NO_x.[72] These reductions were observed for both ambient indoor pollution and pollution generated by air cleaners, with sustained mitigation effects over several months of continuous use. However, the catalyst's lifespan is not indefinite, and its effectiveness declined at varying rates for different pollutants. Specifically, the catalyst's ability to remove NO_x deteriorated more rapidly than its ability to reduce O_3 levels. Based on a 12.5% monotonic decline in the $CADR_{O3}$ observed over a 16-week aging period, we estimate that the catalyst would lose its ability to reduce O_3 pollution after two years of continuous operation. Therefore, the catalyst would need to be replaced more often for sufficient performance. Aging tests of longer duration would be of high interest. For applications where continuous operation is not required, the catalyst's lifespan may be extended. It is possible that the aging rate is influenced by the indoor conditions (e.g. humidity, pollutant concentrations). Observations of NPF from the application of GUV222 lamps in our indoor office were consistent with findings from previous indoor air quality studies.[31, 73-74] While the cause of GUV222-driven NPF is not understood, NPF beyond what is expected from ozonolysis chemistry has been observed under realistic indoor conditions.[73] Since implementation of this catalyst was able to suppress NPF events in addition to removing O_3 pollution, the catalyst could reduce the adverse health effects and mortality associated with air pollution generated by certain air cleaning technologies.

Another important result of this study is that the total impact of the catalyst on VOCs is complex and requires further investigation. While we successfully measured a relatively wide range of VOCs, some VOCs like alkanes are not detected with the instruments we used. More detailed investigation of the fate of individual VOCs upon catalyst processing under varying conditions would be required to further elucidate overall VOC impacts. Even so, current understanding is that PM and O_3 air pollution have a more significant impact on health endpoints and a greater number of disease outcomes than VOCs.[5, 75-77] We therefore conclude that the catalyst has an overall positive impact on indoor air quality and human health, especially when deployed alongside the air disinfection/cleaning methods studied here.

Our results bring attention to the potential advantages of combining technologies to improve indoor air quality, addressing both chemical and biological concerns. Based on the presented findings, we suggest that indoor O_3 and other common indoor air pollutants can be effectively mitigated in real indoor settings using a dedicated catalyst. Continued research is required to evaluate the overall health benefits and risks of different air cleaning and disinfection technologies. Such research will be crucial for informing regulatory guidelines and standards for air cleaners and, more broadly, indoor air quality.

Acknowledgments

We thank Andrew Jensen and Harald Stark for software training and support, and Dongwook Kim and Seonsik Yun for instrument training and support. We thank the Volkamer research group for the use of their rooftop laboratory space. We thank Nadia Tahsini and Jesse Kroll of MIT, Richard Williamson and James Montavon of BluePrint Biosecurity, Vivian Belenky of Columbia University, Shelly Miller, Alberto Garcia, and Karl Linden of CU Boulder, Holger Claus of Ushio, and Aaron Collins and M. Pang of OSLUV for useful discussions. We thank Gregg Sanko from BASF for selling sample catalysts to us. This work was supported by the Kanro Foundation (grant A39) and the Balvi Filantropic Fund (grant A27).

4. References

1. Health Effects Institute. 2024. State of Global Air 2024. Special Report. Boston, MA:Health Effects Institute.

2. Samet, J.M., Spengler, J.D. Indoor environments and health: moving into the 21st century. *American Journal of Public Health*, 93, 9, 1489-1493, https://doi.org/10.2105/AJPH.93.9.1489, 2003.

3. Habre, R., Dorman, D.C., Abbatt, J., Bahnfleth, W.P., Carter, E., Farmer, D., Gawne-Mittelstaedt, G., Goldstein, A.H., Grassian, V.H., Morrison, G., Peccia, J., Poppendieck, D., Prather, K.A., Shiraiwa, M., Stapleton, H.M., Williams, M., Harries, M.E. Why indoor chemistry matters: A national academies consensus report. *Environmental Science & Technology*, 56, 15, 10560-10563, https://doi.org/10.1021/acs.est.2c04163, 2022.

4. Klepeis, N.E., Nelson, W.C., Ott, W.R., Robinson, J.P., Tsang, A.M., Switzer, P., Behar, J.V., Hern, S.C., Engelmann, W.H. The National Human Activity Pattern Survey (NHAPS): a resource for assessing exposure to environmental pollutants. *Journal of Exposure Science & Environmental Epidemiology*, 11, 231-252, https://doi.org/10.1038/sj.jea.7500165, 2001.

5. Bell, M.L., Peng, R.D., Dominici, F. The exposure-response curve for ozone and risk of mortality and the adequacy of current ozone regulations. Environmental Health Perspectives, 114, 532-536, https://doi.org/10.1289/ehp.8816, 2006.

6. Xiang, J., Weschler, C.J., Zhang, J., Zhang, L., Sun, Z., Duan, X., Zhang, Y. Ozone in urban China: Impact on mortalities and approaches for establishing indoor guideline concentrations. *Indoor Air*, 29, 4, 604-615, https://doi.org/10.1111/ina.12565, 2019.

7. He, L., Hao, Z., Weschler, C.J., Li, F., Zhang, Y., Zhang, J.J. Indoor ozone reaction products: Contributors to the respiratory health effects associated with low-level outdoor ozone. *Atmospheric Environment*, 340, 120920, https://doi.org/10.1016/j.atmosenv.2024.120920, 2025.

8. Chen, K., Zhou, L., Chen, X., Bi, J., Kinney, P.L. Acute effect of ozone exposure on daily mortality in seven cities of Jiangsu Province, China: No clear evidence for threshold. *Environmental Research*, 155, 235-241, https://doi.org/10.1016/j.envres.2017.02.009, 2017.

9. Leikauf, G.D. Hazardous air pollutants and asthma. *Environmental Health Perspectives*, 110, 505-526, https://doi.org/10.1289/ehp.02110s4505, 2002.

10. Weschler, C.J. New directions: Ozone-initiated reaction products indoors may be more harmful than ozone itself. *Atmospheric Environment*, 38, 33, 5715-5716, https://doi.org/10.1016/j.atmosenv.2004.08.001, 2004.

11. Wolkoff, P. Indoor air pollutants in office environments: Assessment of comfort, health, and performance. *International Journal of Hygiene and Environmental Health*, 216, 4, 371-394, https://doi.org/10.1016/j.ijheh.2012.08.001, 2013.

12. Nørgaard, A.W., Kofoed-Sørensen, V., Mandin, C., Ventura, G., Mabilia, R., Perreca, E., Cattaneo, A., Spinazzè, A., Mihucz, V.G., Szigeti, T., de Kluizenaar, Y., Cornelissen, H.J.M., Trantallidi, M., Carrer, P., Sakellaris, I., Bartzis, J., Wolkoff, P. Ozone-initiated terpene reaction

products in five European offices: Replacement of a floor cleaning agent. *Environmental Science & Technology*, 48, 22, 13331-13339, https://doi.org/10.1021/es504106j, 2014.

13. Weschler, C.J., Shields, H.C. Indoor ozone/terpene reactions as a source of indoor particles. *Atmospheric Environment*, 33, 15, 2301-2312, https://doi.org/10.1016/S1352-2310(99)00083-7, 1999.

14. Wainman, T., Zhang, J., Weschler, C.J., Lioy, P.J. Ozone and limonene in indoor air: a source of submicron particle exposure. *Environmental Health Perspectives*, 108, 12, 1139-1145, https://doi.org/10.1289/ehp.001081139, 2000.

15. Weichenthal, S., Pinault, L., Christidis, T., Burnett, R.T., Brook. J.R., Chu, Y., Crouse, D.L., Erickson, A.C., Hystad, P., Li, C., Martin, R.V., Meng, J., Pappin, A.J., Tjepkema, M., van Donkelaar, A., Weagle, C.L., Brauer, M. How low can you go? Air pollution affects mortality at very low levels. *Science Advances*, 8, 39, https://doi.org/10.1126/sciadv.abo3381, 2022.

16. Singer, B.C., Coleman, B.K., Destaillats, H., Hodgson, A.T., Lunden, M.M., Weschler, C.J., Nazaroff, W.W. Indoor secondary pollutants from cleaning product and air freshener use in the presence of ozone. *Atmospheric Environment*, 40, 6696-6710, https://doi.org/10.1016/j.atmosenv.2006.06.005, 2006.

17. Peng, Z., Day, D.A., Symonds, G.A., Jenks, O.J., Stark, H., Handschy, A.V., de Gouw, J.A., Jimenez, J.L. Significant Production of Ozone from Germicidal UV Lights at 222 nm. *Environmental Science & Technology Letters*, 10, 8, 668-674, https://doi.org/10.1021/acs.estlett.3c00314, 2023.

18. Long, C.M., Suh, H.H., Catalano, P.J., Koutrakis, P. Using time- and size-resolved particulate data to quantify indoor penetration and deposition behavior. *Environmental Science & Technology*, 35, 2089-2099, https://doi.org/10.1021/es001477d, 2001.

19. Lai, D., Karava, P., Chen, Q. Study of outdoor ozone penetration into buildings through ventilation and infiltration. *Building and Environment*, 93, 2, 112-118, https://doi.org/10.1016/j.buildenv.2015.06.015, 2015.

20. Nazaroff, W.W., Weschler, C.J. Indoor ozone: Concentrations and influencing factors. *Indoor Air*, 32, 1, e12942, https://doi.org/10.1111/ina.12942, 2021.

21. Klompas, M., Milton, D.K., Rhee, C., Baker, M.A., Leekha, S. Current Insights Into Respiratory Virus Transmission and Potential Implications for Infection Control Programs: A Narrative Review. *Annals of Internal Medicine,* 174, 12, https://doi.org/10.7326/M21-2780, 2021.

22. Greenhalgh, T., Jimenez, J.L., Prather, K.A., Tufekci, Z., Fisman, D., Schooley, R. Ten scientific reasons in support of airborne transmission of SARS-CoV-2. *The Lancet*, 397, 10285, 1603-1605, https://doi.org/10.1016/S0140-6736(21)00869-2, 2021.

23. Wang, C.C., Prather, K.A., Sznitman, J., Jimenez, J.L., Lakdwala, S., Tufekci, Z., Marr, L.C. Airborne Transmission of Respiratory Viruses. *Science*, 373, https://doi.org/10.1126/science.abd9149, 2021.

24. Morawska, L., Tang, J.W., Bahnfleth, W., Bluyssen, P.M., Boerstra, A., Buonanno, G., Cao, J., Dancer, S., Floto, A., Franchimon, F., Haworth, C., Hogeling, J., Isaxon, C., Jimenez, J.L., Kurnitski, J., Li, Y., Loomans, M., Marks, G., Marr, L.C., Mazzarella, L., Krikor Melikov, A., Miller, S., Milton, D.K., Nazaroff, W., Nielsen, P.V., Noakes, C., Peccia, J., Querol, X., Sekhar, C., Seppänen, O., Tanabe, S.-I., Tellier, R., Tham, K.W., Wargocki, P., Wierzbicka, A., Yao, M. How can airborne transmission of COVID-19 indoors be minimised? *Environment International*, 142, 105832, https://doi.org/10.1016/j.envint.2020.105832, 2020.

25. Nardell, E.A. Air Disinfection for Airborne Infection Control with a Focus on COVID-19: Why Germicidal UV is Essential. *Photochemistry and Photobiology*, 97, 3, https://doi.org/10.1111/php.13421, 2021.

26. Poppendieck, D., Rim, D., Persily, A.K. Ultrafine Particle Removal and Ozone Generation by In-Duct Electrostatic Precipitators. *Environmental Science & Technology*, 48, 2067-2074, https://doi.org/10.1021/es404884p, 2014.

27. Xiang, J., Weschler, C.J., Mo, J., Day, D., Zhang, J., Zhang, Y. Ozone, Electrostatic Precipitators, and Particle Number Concentrations: Correlations Observed in a Real Office during Working Hours. Environmental Science & Technology, 50, 10236-10244, https://doi.org/10.1021/acs.est.6b03069, 2016.

28. Buonanno, M., Welch, D., Shuryak, I., Brenner, D.J. Far-UVC light (222 nm) efficiently and safely inactivates airborne human coronaviruses. *Scientific Reports*, 10, 1, 10285, https://doi.org/10.1038/s41598-020-67211-2, 2020.

29. Ma, B., Gundy, P.M., Gerba, C.P., Sobsey, M.D., Linden, K.G. UV Inactivation of SARS-CoV-2 across the UVC Spectrum: KrCl* Excimer, Mercury-Vapor, and Light-Emitting Diode (LED) Sources. *Public and Environmental Health Microbiology*, 87, 22, https://doi.org/10.1128/AEM.01532-21, 2021.

30. Blatchley, E.R., Brenner, D.J., Claus, H., Cowan, T.E., Linden, K.G., Liu, Y., Mao, T., Park, S.J., Piper, P.J., Simons, R.M., Sliney, D.H. Far UV-C radiation: An emerging tool for pandemic control. Critical Reviews in Environmental Science and Technology, 53, 6, 733-753, https://doi.org/10.1080/10643389.2022.2084315, 2022.

31. Barber, V.P., Goss, M.B.,Deloya, L.J.F., LeMar, L.N., Li, Y., Helstrom, E., Canagaratna, M., Keutsch, F.N., Kroll, J.H. Indoor Air Quality Implications of Germicidal 222 nm Light. *Environmental Science & Technology*, 57, 42, 15990-15998, https://doi.org/10.1021/acs.est.3c05680, 2023.

32. Link, M.F., Shore, A., Hamadani, B.H., Poppendieck, D. Ozone Generation from a Germicidal Ultraviolet Lamp with Peak Emission at 222 nm. *Environmental Science & Technology Letters*, 10, 8, 675-679, https://doi.org/10.1021/acs.estlett.3c00318, 2023.

33. Peng, Z., Miller, S.L., Jimenez, J.L. Model Evaluation of Secondary Chemistry due to Disinfection of Indoor Air with Germicidal Ultraviolet Lamps. *Environmental Science & Technology Letters*, 10, 1, 6-13, https://doi.org/10.1021/acs.estlett.2c00599, 2023.

34. Jenks, O.J., Peng, Z., Schueneman, M.K., Rutherford, M., Handschy, A.V., Day, D.A., Jimenez, J.L., de Gouw, J.A. Effects of 222 nm germicidal ultraviolet light on aerosol and VOC formation from limonene. *ES&T Air*, 7, 725-733, https://doi.org/10.1021/acsestair.4c00065, 2024.

35. Waring, M. S., Siegel, J. A., Corsi, R. L. Ultrafine particle removal and generation by portable air cleaners. *Atmospheric Environment*, 42, 5003–5014, https://doi.org/10.1016/j.atmosenv.2008.02.011, 2008.

36. Crosley, D. R., Araps, C. J., Doyle-Eisele, M. & McDonald, J. D. Gas-phase photolytic production of hydroxyl radicals in an ultraviolet purifier for air and surfaces. *Journal of the Air & Waste Management Association*, 67, 231–240, https://doi.org/10.1080/10962247.2016.1229236, 2017.

37. Ratliff, K.M., Oudejans, L., Archer, J., Calfee, W., Gilberry, J.U., Hook, D.A., Schoppman, W.E., Yaga, R.W., Brooks, L., Ryan, S. Large-scale evaluation of microorganism inactivation by bipolar ionization and photocatalytic devices. *Building and Environment*, 227, 1, 109804, https://doi.org/10.1016/j.buildenv.2022.109804, 2023.

38. Collins, D.B., Farmer, D.K. Unintended Consequences of Air Cleaning Chemistry. *Environmental Science & Technology*, 55, 12172-12179, https://doi.org/10.1021/acs.est.1c02582, 2021.

39. Weschler, C.J., Shields, H.C., Naik, D.V. Ozone-removal efficiencies of activated carbon filters after more than three years of continuous service. *ASHRAE Transactions: Symposia*, 100, 2, 1121-1129, 1994.

40. Ryhl-Svendsen, M. and Clausen, G. The Effect of Ventilation, Filtration and Passive Sorption on Indoor Air Quality in Museum Storage Rooms. *Studies in Conservation*, 54, 1, https://doi.org/10.1179/sic.2009.54.1.35, 2009.

41. Kunkel, D.A., Gall, E.T, Siegel, J.A., Novoselac, A., Morrison, G.C., Corsi, R.L. Passive reduction of human exposure to indoor ozone. *Building and Environment*, 45, 2, 445-452, https://doi.org/10.1016/j.buildenv.2009.06.024, 2010.

42. Namdari, M., Lee, C.-S., Haghighat, F. Active ozone removal technologies for a safe indoor environment: a comprehensive review. *Building and Environment*, 187, 107370, https://doi.org/10.1016/j.buildenv.2020.107370, 2021.

43. Tang, M., Siegel, J.A., Corsi, R.L., Novoselac, A. Evaluation of ozone removal devices applied in ventilation systems. *Building and Environment*, 225, 109582, https://doi.org/10.1016/j.buildenv.2022.109582, 2022.

44. Jia, J., Zhang, P., Chen, L. Catalytic decomposition of gaseous ozone over manganese dioxides with different crystal structures. *Applied Catalysis B: Environmental*, 189, 210-218, https://doi.org/10.1016/j.apcatb.2016.02.055, 2016.

45. Spöri, C., Kwan, J.T.H., Bonakdarpour, A., Wilkinson, D.P., Strasser, P. The stability challenges of oxygen evolving catalysts: Towards a common fundamental understanding and

mitigation of catalyst degradation. *Angewandte Chemie International Edition*, 56, 22, 5994-6021, https://doi.org/10.1002/anie.201608601, 2016.

46. Wang, Y., Ge, C., Zhan, L., Li, C., Qiao, W., Ling, L. MnO_x-CeO_2/activated carbon honeycomb catalyst for selective catalytic reduction of NO with NH_3 at low temperatures. *Industrial & Engineering Chemistry Research*, 51, 36, 11667-11673, https://doi.org/10.1021/ie300555f, 2012.

47. Liu, J., Guo, R., Li, M., Sun, P., Liu, S., Pan, W., Liu, S., Sun, X. Enhancement of the SO_2 resistance of Mn/TiO_2 SCR catalyst by Eu modification: A mechanism study. *Fuel*, 223, 385-393, https://doi.org/10.1016/j.fuel.2018.03.062, 2018.

48. Meng, D., Xu, Q., Jiao, Y., Guo, Y., Guo, Y., Wang, L., Lu, G., Zhan, W. Spinel structured $Co_aMn_bO_x$ mixed oxide catalyst for the selective catalytic reduction of NO_x with NH_3. *Applied Catalysis B: Environmental*, 221, 652-663, https://doi.org/10.1016/j.apcatb.2017.09.034, 2018.

49. Han, L., Cai, S., Gao, M., Hasegawa, J., Wang, P., Zhang, J., Shi, L., Zhang, D. Selective catalytic reduction of NO_x with NH_3 by using novel catalysts: State of the art and future prospects. *Chemical Reviews*, 119, 10916-10976, https://doi.org/10.1021/acs.chemrev.9b00202, 2019.

50. Sekine, Y. Oxidative decomposition of formaldehyde by metal oxides at room temperature. *Atmospheric Environment*, 36, 35, 5543-5547, https://doi.org/10.1016/S1352-2310(02)00670-2, 2002.

51. Sidheswaran, M.A., Destaillats, H., Sullivan, D.P., Larsen, J., Fisk, W.J. Quantitative room-temperature mineralization of airborne formaldehyde using manganese oxide catalysts. *Applied Catalysis B: Environmental*, 107, 34-41, https://doi.org/10.1016/j.apcatb.2011.06.032, 2011.

52. Destaillats, H., Sidheswaran, M., Cohn, S., Sullivan, D.P., Fisk, W.J. Laboratory and Field Demonstration of Energy Efficient VOC Removal Using a Manganese Oxide Catalyst at Room Temperature. *LBL Publications*, https://escholarship.org/uc/item/3kb3m7mv, 2014.

53. Zhu, S., Wang, J., Nie, L. Progress of Catalytic Oxidation of Formaldehyde over Manganese Oxides. *ChemistrySelect*, 4, 41, 12085-12098, https://doi.org/10.1002/slct.201902701, 2019.

54. Zheng, J., Zhao, W., Song, L., Wang, H., Yan, H., Chen, G., Han, C., Zhang, J. Advances of manganese-oxides-based catalysts for indoor formaldehyde removal. *Green Energy & Environment*, 8, 3, 626-653, https://doi.org/10.1016/j.gee.2022.01.008, 2023.

55. Krechmer, J.E., Day, D.A., Ziemann, P.J., Jimenez, J.L. Direct measurements of gas/particle partitioning and mass accommodation coefficients in environmental chambers. *Environmental Science & Technology*, 51, 20, 11867-11875, https://doi.org/10.1021/acs.est.7b02144, 2017.

56. Day, D. A., Fry, J. L., Kang, H. G., Krechmer, J. E., Ayres, B. R., Keehan, N. I., Thompson, S. L., Hu, W., Campuzano-Jost, P., Schroder, J. C., Stark, H., DeVault, M. P., Ziemann, P. J., Zarzana, K. J., Wild, R. J., Dubè, W. P., Brown, S. S., Jimenez, J. L. Secondary organic aerosol mass yields from NO_3 oxidation of α-pinene and Δ-carene: Effect of RO_2 radical fate. *The*

Journal of Physical Chemistry A, 126, 40, 7309-7330, https://doi.org/10.1021/acs.jpca.2c04419, 2022.

57. Manuja, A., Ritchie, J., Buch, K., Wu, Y., Eichler, C.M.A., Little, J.C., Marr, L.C. Total surface area in indoor environments. *Environmental Science: Processes & Impacts*, 21, 1384-1392, https://doi.org/10.1039/C9EM00157C, 2019.

58. Nazaroff, W.W. Residential air-change rates: A critical review. *Indoor Air*, 31, 2, 282-313, https://doi.org/10.1111/ina.12785, 2021.

59. Day, D.A., Cubison, M.J., Palm, B.B., Yun, S., J.L. Jimenez Research Group, Scanning Mobility Particle Sizer Loader and Plotter, University of Colorado, Boulder. Available at: https://gitlab.com/JimenezGroup/jg-utilities. Date accessed: 30 July, 2024.

60. Lee, B.H., Lopez-Hilfiker, F.D., Mohr, C., Kurtén, T., Worsnop, D.R., Thornton, J.A. An iodide-adduct high-resolution time-of-flight chemical-ionization mass spectrometer: Application to atmospheric inorganic and organic compounds. *Environmental Science & Technology*, 48, 11, 6309-6317, https://doi.org/10.1021/es500362a, 2014.

61. Jensen, A., Liu, Z., Tan, W., Dix, B., Chen, T., Koss, A., Zhu, L., Li, L., de Gouw, J.A. Measurements of volatile organic compounds during the COVID-19 lockdown in Changzhou, China. *Geophysical Research Letters*, 48, 20, e2021GL095560, https://doi.org/10.1029/2021GL095560, 2021.

62. Rutherford, M., Koss, A., de Gouw, J.A. Mobile VOC measurements in Commerce City, CO reveal the emissions from different sources. *Journal of the Air & Waste Management Association*, 74, 10, https://doi.org/10.1080/10962247.2024.2379927, 2024.

63. Krechmer, J., Lopez-Hilfiker, F., Koss, A., Hutterli, M., Stoermer, C., Deming, B., Kimmel, J., Warneke, C., Holzinger, R., Jayne, J., Worsnop, D., Fuhrer, K., Gonin, M., de Gouw, J. Evaluation of a new reagent-ion source and focusing ion-molecule reactor for use in proton-transfer-reaction mass spectrometry. *Analytical Chemistry*, 90, 12011-12018, https://doi.org/10.1021/acs.analchem.8b02641, 2018.

64. Koss, A.R., Sekimoto, K., Gilman, J.B., Selimovic, V., Coggon, M.M., Zarzana, K.J., Yuan, B., Lerner, B.M., Brown, S.S., Jimenez, J.L., Krechmer, J., Roberts, J.M., Warneke, C., Yokelson, R.J., de Gouw, J. Non-methane organic gas emissions from biomass burning: identification, quantification, and emission factors from PTR-ToF during the FIREX 2016 laboratory experiment. *Atmospheric Chemistry and Physics*, 18, 3299-3319, https://doi.org/10.5194/acp-18-3299-2018, 2018.

65. Pagonis, D., Sekimoto, K., de Gouw, J. A library of proton-transfer reactions of H_3O^+ ions used for trace gas detection. *Journal of the American Society for Mass Spectrometry*, 30, 1330-1335, https://doi.org/10.1007/s13361-019-02209-3, 2019.

66. Hansel, A., Singer, W., Wisthaler, A., Schwarzmann, M., Lindinger, W. Energy dependencies of the proton transfer reactions $H_3O^+ + CH_2O \longleftrightarrow CH_2OH^+ + H_2O$. *International Journal of Mass Spectrometry and Ion Processes*, 167-168, 697-703, https://doi.org/10.1016/S0168-1176(97)00128-6, 1997.

67. Wisthaler, A., Apel, E.C., Bossmeyer, J., Hansel, A., Junkermann, W., Koppmann, R., Meier, R., Müller, K., Solomon, S.J., Steinbrecher, R., Tillman, R., Brauers, T. Technical note: Intercomparison of formaldehyde measurements at the atmospheric simulation chamber SAPHIR. *Atmospheric Chemistry and Physics*, 8, 2189-2200, https://doi.org/10.5194/acp-8-2189-2008, 2008.

68. Yuan, B., Koss, A.R., Warneke, C., Coggon, M., Sekimoto, K., de Gouw, J.A. Proton-transfer-reaction mass spectrometry: Applications in atmospheric sciences. *Chemical Reviews*, 117, 21, 13187-13229, https://doi.org/10.1021/acs.chemrev.7b00325, 2017.

69. Link, M.F., Robertson, R., Claflin, M.S., Poppendieck, D. Quantification of byproduct formation from portable air cleaners using a proposed standard test method. *Environmental Science & Technology*, 58, 18, 7916-7923, https://doi.org/10.1021/acs.est.3c09331, 2024.

70. Pappas, G.P., Herbert, R.J., Henderson, W., Koenig, J., Stover, B., Barnhart, S. The respiratory effects of volatile organic compounds. *International Journal of Occupational and Environmental Health*, 6, 1, 1-8, https://doi.org/10.1179/oeh.2000.6.1.1, 2000.

71. Perna, R.B., Bordini, E.J., Deinzer-Lifrak, M. A case of claimed persistent neuropsychological sequelae of chronic formaldehyde exposure clinical, psychometric, and functional findings. *Archives of Clinical Neuropsychology*, 16, 1, 33-44, https://doi.org/10.1093/arclin/16.1.33, 2001.

72. Logue, M.J., Klepeis, N.E., Lobscheid, A.B., Singer, B.C. Pollutant exposures from natural gas cooking burners: A simulation-based assessment for Southern California. *Environmental Health Perspectives*, 122, 43-50, https://doi.org/10.1289/ehp.1306673, 2013.

73. Goss, M.B., Kroll, J.H. Organic aerosol formation from 222 nm germicidal light: ozone-initiated vs. non-ozone pathways. *Environmental Science: Processes and Impacts*, https://doi.org/10.1039/D4EM00384E, 2024.

74. Link, M.F., Robertson, R.L., Shore, A., Hamadani, B.H., Cecelski, C.E., Poppendieck, D.G. Ozone generation and chemistry from 222 nm germicidal ultraviolet light in a fragrant restroom. *Environmental Science: Processes & Impacts*, 26, 1090-1106, https://doi.org/10.1039/D4EM00144C, 2024.

75. Anenberg, S.C., Horowitz, L.W., Tong, D.Q., West, J.J. An estimate of the global burden of anthropogenic ozone and fine particulate matter on premature human mortality using atmospheric modeling. *Environmental Health Perspectives*, 118, 9, 1189-1195, https://doi.org/10.1289/ehp.0901220, 2010.

76. Lepuele, J., Laden, F., Dockery, D., Schwartz, J. Chronic exposure to fine particles and mortality: An extended follow-up of the Harvard Six Cities Study from 1974 to 2009. *Environmental Health Perspectives*, 120, 7, 965-970, https://doi.org/10.1289/ehp.1104660, 2012.

77. Kelly, F.J., Fussell, J.C. Air pollution and public health: emerging hazards and improved understanding of risk. *Environmental Geochemistry and Health*, 37, 631-649, https://doi.org/10.1007/s10653-015-9720-1, 2015.

For Table of Contents Only: